Heliyon 10 (2024) e28978

Contents lists available at ScienceDirect

Heliyon

journal homepage: www.cell.com/heliyon

Research article

A comparison of traditional and net structured intersomatic cages in the lombosacral region: A biomechanical analysis for enhancing discopathy treatment

Filippo Cucinotta [a], Rosalia Mineo [b], Marcello Raffaele [a,*], Fabio Salmeri [a], Fulvio Tartara [c], Felice Sfravara [a]

[a] *Department of Engineering, University of Messina, Italy*
[b] *Mt Ortho S.r.l, Italy*
[c] *Istituto Clinico Città Studi, Milano, Italy*

A R T I C L E I N F O

Keywords:
Magnetic resonance imaging
Biomedical computer aided design
Range of motion
CAE method

A B S T R A C T

The vertebral column represents an essential element for support, mobility, and the protection of the central nervous system. Various pathologies can compromise these vital functions, leading to pain and a decrease in the quality of life. Within the scope of this study, a novel redesign of the Intersomatic Cage, traditionally used in the presence of discopathy, was proposed. The adoption of additive manufacturing technology allowed for the creation of highly complex geometries, focusing on the lumbosacral tract, particularly on the L4-L5 and L5-S1 intervertebral discs. In addition to the tensile analysis carried out using Finite Element Analysis (FEA) in static simulations, a parallel study on the range of motion (ROM) of the aforementioned vertebral pairs was conducted. The ROM represents the relative movement range between various vertebral pairs. The introduction of the intersomatic cage between the vertebrae, replacing the pulpy nucleus of the intervertebral disc, could influence the ROM, thus having significant clinical implications. For the analysis, the ligaments were modelled using a 1D approach. Their constraint reaction and deformability upon load application were analysed to better understand the potential biomechanical implications arising from the adoption of the cages. During the FEA simulations, two types of cages were analysed: LLIF for L4-L5 and ALIF for L5-S1, subjecting them to four different loading conditions. The results indicate that the stresses exhibited by cages with a NET structure are generally lower compared to those of traditional cages. This stress reduction in cages with NET structure suggests a more optimal load distribution, but it is essential to assess potential repercussions on the surrounding bone structure.

1. Introduction

The spine is an important anatomical structure that plays a fundamental role in support, mobility, and protection of the central nervous system. Unfortunately, a range of disorders and diseases can compromise the integrity and functioning of the spine, leading to pain, disability, and a reduced quality of life. Among these conditions are intervertebral disc herniation, spinal stenosis,

* Corresponding author.
E-mail addresses: filippo.cucinotta@unime.it (F. Cucinotta), rosalia.mineo@mtortho.com (R. Mineo), marcello.raffaele@unime.it (M. Raffaele), fabio.salmeri@unime.it (F. Salmeri), tartarafulvio@gmail.com (F. Tartara), felice.sfravara@unime.it (F. Sfravara).

https://doi.org/10.1016/j.heliyon.2024.e28978
Received 29 July 2023; Received in revised form 27 March 2024; Accepted 27 March 2024
Available online 4 April 2024

spondylolisthesis, and vertebral fractures. Degenerative lumbar disc disease is a topic of growing interest, especially considering the increasing life expectancy and ageing of the population. An article by Saleem et al. [1] delved deeply into the prevalence and characteristics of this condition. According to the research, back pain is one of the most common global ailments and often originates from lumbar disc degeneration, particularly due to disc herniations. Using magnetic resonance imaging, a non-invasive and highly effective tool, the authors were able to observe and describe the lumbar spine in detail. One intriguing discovery pertains to susceptibility to degeneration: men appear to be more affected than women, likely due to increased mechanical strains and injuries. Age plays a pivotal role in the distribution of lesions. While older patients tend to develop degenerations at the upper lumbar levels (such as L1-L2, L2-L3, L3-L4), younger individuals display degenerations at the lower levels (L4-L5 and L5-S1). This detail is crucial as it suggests that the L4-L5 and L5-S1 zones are particularly vulnerable. One of the article's most salient revelations is the frequent presence of degeneration at levels L4-L5 and L5-S1. These areas show the highest rates of degeneration, affirming the notion that these zones are particularly exposed to mechanical stresses and thus at greater risk. In summary, the study by Saleem et al. provides valuable insights into degenerative lumbar disc disease, emphasising the importance of prevention and awareness. Through a detailed understanding of the mechanisms and most affected areas, it's possible to develop more effective strategies for the condition's management and treatment.

Over the years, research and clinical practice have led to the development of various treatment techniques aimed at restoring stability and proper functioning of the spine. One of the main challenges in treating spinal disorders involves restoring the disc height between the vertebrae. Maintaining disc height is crucial for ensuring proper load distribution on the vertebrae and preventing further damage to the intervertebral discs and surrounding structures. Moreover, adequate disc height is essential for maintaining mobility and function of spinal joints.

Among the various treatment approaches for spine stabilization, the Lateral Mass Screw (LMS) is an established method used for treating a wide range of spinal conditions. This surgical technique, originally described by Roy-Camille in 1970 [2], involves inserting stabilization screws into the lateral mass of cervical, thoracic, or lumbar vertebrae to secure bone structures and reduce the mobility of the involved vertebrae [3,4]. Another modern and widely used clinical approach for most cases of discopathies is the use of Intersomatic Cages. These are interbody fusion devices that are inserted between the vertebrae to restore disc height and promote bone fusion. These devices are made from various materials, such as titanium [5], PEEK, or biocompatible materials, and can be customized to fit the size and shape of the patient's vertebrae. These are typically constructed using additive manufacturing (AM) [6,7] techniques and rapid prototyping (RP) [8].

The potential clinical benefits of this research relate to a comprehensive understanding of how intervertebral cages with net structures might influence the biomechanical properties of the spine, potentially providing improved solutions for patients with spinal issues. One must remember that damage to ligaments, vertebral joints, and muscles often result from degenerative changes. These alterations can lead to increased susceptibility to injuries and chronic pain, involving both the spinal nerve roots and the neural endings in the inflamed and degenerated disc [9]. Importantly, an excess of tension on the vertebra's surface can lead to stress concentration. Over time, this can give rise to microfractures, which can eventually result in the mechanical failure of the vertebra. It's worth noting a particularly relevant study by Timothy L. Siu et al. [10], this work delved into the complexities of treating osteoporotic fractures and the associated vertebral deformities. In a notable case description, a 74-year-old woman presented with osteoporotic fractures at L2 and L3, resulting in a concave deformity of the end plates. The challenges posed by her specific anatomy, especially the concave deformity, made conventional off-the-shelf implants incompatible. However, leveraging in silico simulations based on preoperative CT scans, they designed and manufactured customized titanium cages through 3D additive manufacturing. The outcome was promising, as postoperative assessments showcased excellent alignment between the implants and the patient's anatomy, resulting in symptom resolution and evidence of interbody fusion by the 6-month follow-up. Drawing from the insights of such studies, the design and application of intervertebral cages can play a pivotal role in addressing these risks. However, these interventions must be approached with caution, ensuring that the biomechanical impacts they might introduce are carefully considered. The overarching aim is to ensure that these interventions are implemented in the safest and most effective manner in clinical practice.

This paper aims to discuss and analyze the reengineering of a traditional Intersomatic Cage taking advantage of computer aided methods and the possibility, thanks to Additive Manufacturing, to develop complex pattern for improving the beneficial effects of these devices. The objective of this approach is to evaluate, in the post-operative period and after that osteointegration has occurred, how the different cages interact with the patient's vertebrae and the imprint left on the vertebral surfaces [11]. This comparative analysis between different cages will allow for a better understanding of the biomechanical and biological dynamics involved in the spinal fusion process, as well as identifying any differences in performance and effectiveness of the various types of interbody devices. The first step was the reconstruction of the lumbosacral tract through a segmentation process starting from a magnetic resonance imaging scan. The study's aim is to verify and compare the stresses generated on the bone surface of the vertebrae when different types of intervertebral arthroplasty devices are inserted. Two clinical cases of discopathy involving two different subjects, with issues at L4-L5 and L5-S1 respectively, were studied. Both cases will be treated with two types of cages: LLIF (Lateral Lumbar Interbody Fusion) for the L4-L5 case and ALIF (Anterior Lumbar Interbody Fusion) for the L5-S1 case. The cage reengineered is produced by MtOrtho©, which use an internal structure called NET, and the traditional one is produced by another manufacturer without the NET internal structure. The results obtained from this study could help to better understand the implications of using arthroplasty prostheses in the spine with or without NET and potentially improve the quality of treatment for patients suffering from discopathies.

2. Materials and methods

2.1. Anatomy of the lower part of the spine and diseases

The study proposed in the article focuses on the effects on the bone structures caused by the application of arthroprosthetic prostheses in cases of discopathy. The application of the study is principally focused on the lumbosacral tract of the spine. The first step has been the reconstruction of the lumbosacral tract. The CAD model was obtained through a process of segmentation starting from a magnetic resonance. The software used is InVesalius version 3.1. Once the MRI (Magnetic Resonance Imaging) in DICOM format is imported, a specific type of tissue has been used for the segmentation process. The thresholding segmentation technique detects only the pixels whose intensity falls within the threshold range defined by the user. Finally, the surfaces are created using the marching cubes algorithm, which converts voxels from segmented images into polygons (triangles) [12]. The MRI images belong to an adult male with a height of 171.4 cm and with a weight of 63.3 kg. The spinal column has a fundamental function for our body: it supports the weight of the body, allows movement and protects the spinal cord. The lumbosacral area, in particular, refers to the lower part of the spine, which consists of the lumbar and sacral vertebrae. These vertebrae are L4 and L5 for the lumbar part and S1 for the sacral region, as shown in (Fig. 1), which includes (Fig. 1a): a frontal view (Fig. 1b), a lateral view (Fig. 1c), a sagittal section, and (Fig. 1d) the scientific nomenclature. Also the posterior part of the column has been modelled and used for the simulations.

The intervertebral disc is a structure located between the vertebrae of the spinal column. It consists of a central nucleus, called the nucleus pulposus, and an outer ring of fibrous tissue called the annulus fibrosus. The nucleus pulposus consists of a gelatinous substance, while the fibrous ring consists of collagen and elastic fibres. This structure is important because it acts as a cushion between the vertebrae, allowing to absorb shocks and pressure on the spine during body movements. Diseases that can affect the intervertebral disc include disc herniation, disc degeneration and spinal stenosis. A herniated disc occurs when the inner core of the disc protrudes from its normal position and compresses the surrounding spinal nerve roots. Disc degeneration is a condition in which the disc loses its elasticity and water content, becoming less able to absorb the forces acting on the spinal column. Spinal stenosis occurs when the space within the spinal canal narrows, putting pressure on the spinal cord and nerve roots. When the intervertebral disc deteriorates or ruptures, it can cause pain and dysfunction in the spine. All these diseases usually are treated with an intervertebral fusion, it is considered the main treatment for spinal instability. With this method, part of the vertebrae and soft tissues of the disc are partially removed, in medical terms “bleeding the bone” so as to promote osseointegration. At the end of the bleeding the bone process the only part of the disc left between vertebrae is the annulus since the pulposus part is completely removed to make room for the insertion of the cage device. The most important step of this treatment is the insertion of an intervertebral cage in place of the nucleus pulposus in order to keep an healthy vertebral space, restore the height of the spine and maintain a physiological curvature. The surgery and subsequent implantation of course reduce the pain of the patient but it can have undesirable consequences on movement. In fact, with the insertion of the cage there might be a reduction in range of motion (ROM) in the three directions: flexion, flexion-extension, and axial rotation [13] (Fig. 2).

2.2. MtOrtho device, NET structure description and case studies

As mentioned above, one of the most important step of the treatment is the insertion of the cage. The treatment of this problem is addressed with this technique that stimulates lumbar interbody fusion, with the aim of supporting and stabilizing the spine by restoring the height of the disc. The device that stimulates this fusion, developed by Bagdy in the 80s [14] is currently referred to as an interbody cage. This spinal interbody cage is a small porous and hollow implant, of different shapes, which replaces the degenerated disc between two vertebrae, bringing them back to their physiological height. Bone grafts can be placed inside the hollow or porous cage stimulating bone growth through the cage, promoting bone fusion between the affected vertebrae. The cartilaginous endplates of the bone are scraped to help the engagement of the cages (this process is sometimes referred to as "bleeding the bone"). As for the intervertebral disc,

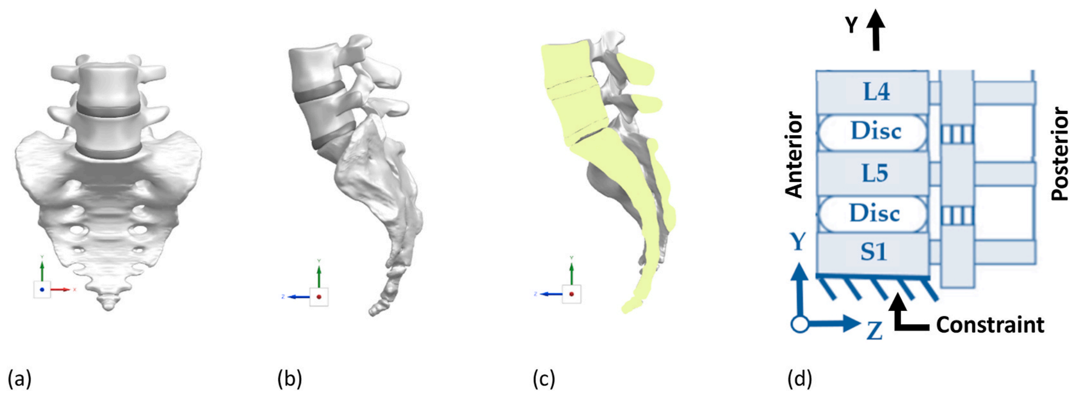

Fig. 1. 3D polygonal reconstruction of the lumbosacral spine: (**a**) frontal view, (**b**) lateral view, (**c**) sagittal section and (**d**) the scientific nomenclature.

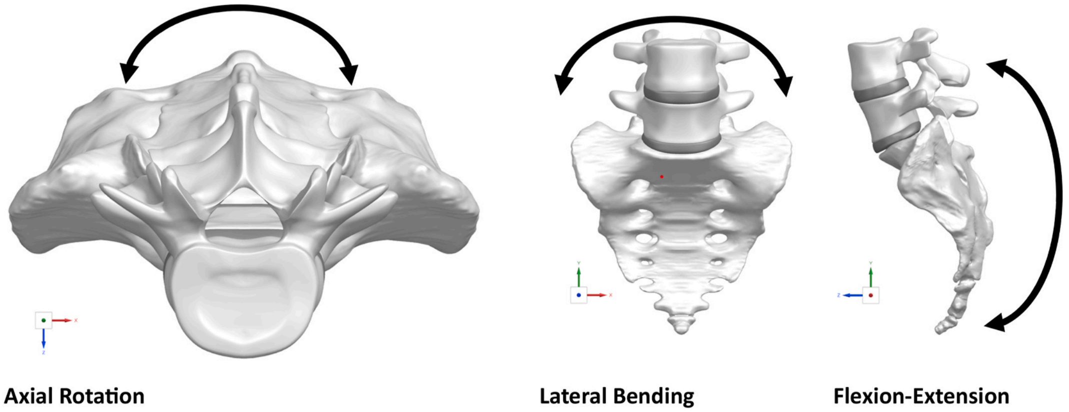

Fig. 2. Definition of range of motion.

the nucleus pulposus, with part of the annulus, is removed to make space for the cage. The case studies reported in the paper concern the pairs of vertebrae L4-L5 and L5-S1. In the first case, the cage normally used is the Lateral Lumbar Interbody Fusion (LLIF), in the second case the cage used is Anterior Lumbar Interbody Fusion (ALIF). The different nomenclature indicates a different type of access and consequently of implantation of the cage. Resuming the two cases studied.

- LLIF, used in the L4-L5 pair with lateral access to the intervertebral disc.
- ALIF, used in the L5-S1 pair with anterior access to the intervertebral disc.

The cage usually has a supporting structure called “melt”. This structure allows to keep the distance between the vertebrae.

Usually, this kind of cages have a low capacity of load absorption and they make difficult to help the osseointegration. In order to improve the strength and stability of the spine (increasing the surface of the load application) and in order to increase the possibility to have osseointegration, the two original cages have been reengineered with a “net” structure inside the melt supporting structure. The melt structure has been modified to insert the “net” structure in Fig. 3, which displays (Fig. 3a): case 1 LLIF configuration without net (Fig. 3b); case 2 LLIF configuration with net (Fig. 3c); case 3 ALIF configuration without net (Fig. 3d); case 3 ALIF configuration with net. The research by Caliogna et al. (2020) [15] clearly demonstrated the efficacy of trabecular titanium, produced using EBM technology, in promoting the adhesion, migration, and proliferation of human adipose-derived stem cells (hASCs) without the need to chemically or physically modify the scaffold’s surface. The specific design of these cages has been shown to have the capacity to trigger osteogenic differentiation, a crucial starting point in understanding the mechanism of osteoinduction [16]. From a biological behaviour standpoint, the highly porous metal cages produced with EBM technology, resembling trabecular bone, appear to offer significant osteoinductive capability and strong potential for bone regeneration. These properties are underscored by the results obtained in in vitro studies. However, it is essential to emphasise that, despite these promising properties of the cages, an in vivo investigation is required to confirm their osteointegration and osteoinduction capabilities. In summary, the use of a NET structure in intersomatic cages can offer substantial benefits in terms of osteointegration and vertebral fusion. This material, produced with EBM technology, is not only biocompatible and promotes cell adhesion and proliferation, but has also shown to trigger osteogenic differentiation. This makes it potentially ideal for clinical applications in patients with discopathy, although further in vivo research is needed to fully confirm these findings. The net structure is a dodecahedral lattice structure [17].

By means of static FEA simulations, two clinical cases of discopathy involving two different subjects, with problems at L4-L5 and L5-S1 respectively, were studied. Both cases will be treated with two types of cages: LLIF (Lateral Lumbar Interbody Fusion) for the L4-L5 case and ALIF (Anterior Lumbar Interbody Fusion) for the L5-S1 case. The comparison will be between the cages produced by

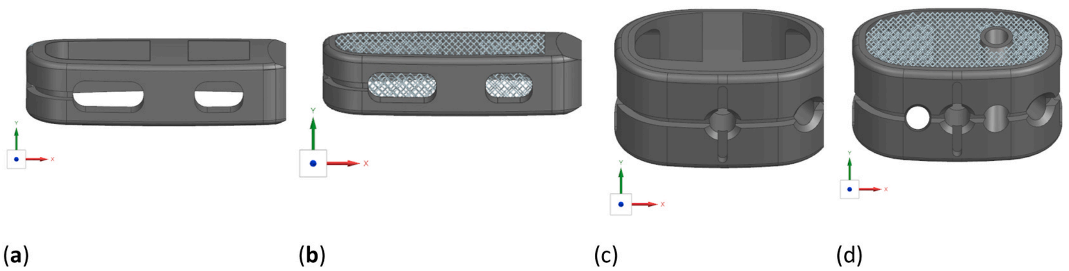

Fig. 3. **a**) case 1 LLIF configuration without net; (**b**) case 2 LLIF configuration with net; (**c**) case 3 ALIF configuration without net; (**d**) case 3 ALIF configuration with net.

MtOrtho, which use the internal structure called NET (case B and D), and those produced by another manufacturer without the internal NET structure (case A and C). Fig. 4 shows the workflow of the case studies. Starting from the same clinical case, the first turning point is the position of discopathy, respectively L4-L5 and L5-S1, along the path the second important turning point is the evaluation of the cage with and without reengineering (respectively without and with net structure).

The study carried out has the purpose of verifying and comparing the level of von Mises stress on the bone surface of the vertebrae when a different type of arthroprosthetic device is inserted. In particular it is very important evaluate the level of stress in different position of the vertebrae identifying the maximum value and the position of this value, the distribution of the pressure on the cage and the area affected by this pressure. In addition, it is very important to define a computer aided method for evaluating the efficiency of different solution of cages. The section of the vertebral column considered is the lumbar-sacral section, as specified above, the pairs of vertebrae L4-L5 and L5-S1.

2.3. Simulation – mechanical properties, constraint system, contacts and methods

The FEA simulations are made with the Siemens© Nx 1859 software. To make the comparison, 4 basic models were created. Respectively the LLIF without net (case A), the LLIF with net (case B), the ALIF without net (case C) and the ALIF with net (case D), as shown in Fig. 3 (a-b-c-d). The melt and the net of the cages are made by Additive Manufacturing (AM) EBM in Ti–6Al–4V ELI, whose mechanical characteristics, treated as isotropic and homogeneous, are shown in Table 1 [18].

The possibility to manufact with AM method allows to use particular design that could improve both the mechanically behavior of the cage and the process of osteointegration. The net was realized as a lattice structure with a rhombic dodecahedral repeated pattern, it is repeated until to fill the volume inside the melt structure. As shown in Fig. 5, the single cell is made with beams structure and the diameter of the beams is constant and it is equal to $D = 0.2$ mm. The enveloping cube of the single cell has two different dimensions in function of the position of the cell inside the volume to fill. The cells along the surface of the net, structure in contact with the bone, has a dimension of $L = 2$ mm, the cells that are not directly in contact with the bone have a dimension of $L = 3$ mm, as shown in Fig. 5(b and c).

This difference is very important in order to increase the possibility of osteointegration, indeed the cells with a dimension of 3 mm are filled with the residual material of the bone after the bleeding operation. As a model of the lumbar spine has been used a CAD model obtained through the segmentation method. The starting point of the process was the magnetic resonance of a male subject of average height. The spine model consists of the following parts.

- L4-L5-S1 vertebrae (cortical and cancellous part)
- Posterior structure
- Residual annulus, after removal following the implantation of the cages
- Anterior longitudinal ligament, ALL
- Posterior longitudinal ligament, PLL
- Flavum ligament, FL
- Interspinous ligament, ISL
- Supraspinous ligament, SSL
- Capsular ligament, CL

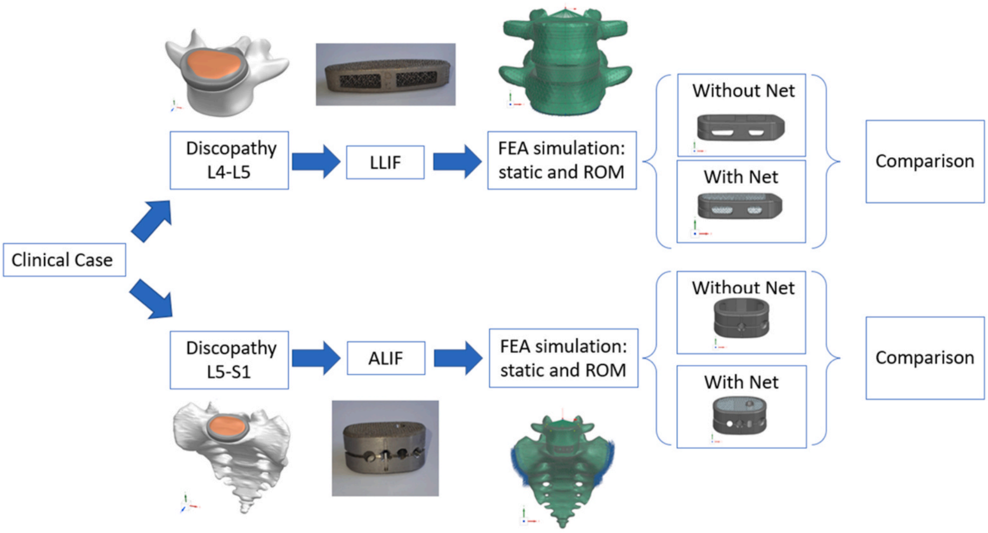

Fig. 4. The case study: Workflow.

Table 1
Mechanical characteristics of the materials of the various cage structures (Melt and Net).

Cage	Yield stress, $\sigma_{y\ 0.2\%}$ [MPa]	Tensile strength σ_m [MPa]	Young's Modulus E [GPa]
Melt	885	895	118
	Compressive strength σ_c [MPa]	Crush strength σ_{cs} [MPa]	Young's Modulus E [MPa]
Net	39.9	29.4	1104

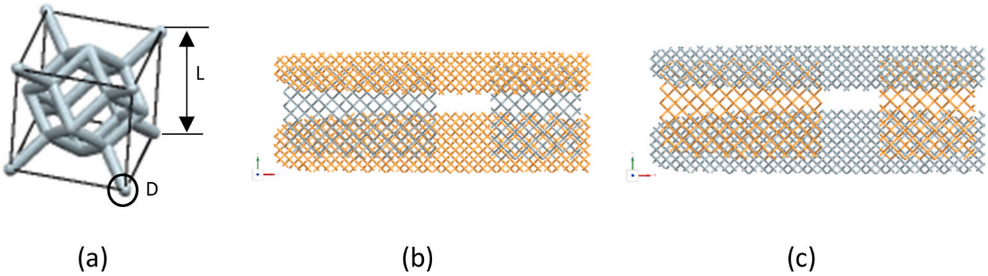

Fig. 5. The dimensions of the "L" side of the enveloping cube and the "D" diameter of the beam element (**a**), in image (**b**) the surface net with dimensions L = 2 mm is highlighted in orange, instead in image (**c**) the NET with L = 3 mm is highlighted in orange.

The bone material of the vertebrae consists of two parts, cortical and cancellous. The mechanical properties have been modelled as a homogeneous and isotropic material [19,20,21,22,23,24,25,26,27,28]. There are different approaches in literature for modelling the cortical and cancellous structure, some authors use orthotropic models, however, in the scientific literature the simplification to isotropic material is widely used [29,30,31,32,33,34,35,26,36]. Table 2 shows the mechanical properties used during the simulation.

The remaining annulus was modelled as a hyperelastic solid with mechanical properties given by the Mooney-Rivlin theory [37,38]. The new Poisson's coefficient (1) is calculated knowing the C_{10} and C_{01} coefficients that are tabulated in the literature [39]. The Poisson coefficient (Eq. (2.1)) will depend on two other coefficients, namely structural damping (Eq. (2.2)) and volumetric deformation (Eq. (2.3)) [40].

$$\upsilon = \frac{3K - 2G}{6K + 2G} \tag{Eq. 2.1}$$

$$G = 2(C_{10} + C_{01}) \tag{Eq. 2.2}$$

$$K = 1000\,(C_{10} + C_{01}) \tag{Eq. 2.3}$$

Thanks to the considerations explained above, the mechanical characteristics of the annulus are summarized in Table 3.

The ligaments were modelled with two-node CROD connection elements by defining the Young's modulus, Poisson's modulus and cross-sectional area per element. The elements were arranged in the anatomical direction given in the literature [41] (Table 4).

The CAD model was discretized using the mesh, as shown in Fig. 6, which depicts: the CAD models of L4-L5 (Fig. 6a) and L5-S1 (Fig. 6c) and the FEM model of L4-L5 (Fig. 6b) and L5-S1 (Fig. 6d). To isolate the results of the Finite Element Analysis (FEA) from the mesh size, different mesh dimensions were established for the vertebrae and the intersomatic CAGE device. For the vertebrae, meshes of 1 mm, 3 mm and 7 mm were used. As for the intersomatic CAGE device and annulus, the mesh dimensions used were 0.5 mm, 1 mm and 3 mm. In detail, for the vertebrae, the low-quality mesh (element size 7 mm, number of elements 106411, number of nodes 21458), medium-quality mesh (element size 3 mm, number of elements 137795, number of nodes 29362) and high-quality mesh (element size 1 mm, number of elements 359867, number of nodes 82288), were characterised by a progressive decrease in element size and an increase in the number of elements and nodes.

For the intersomatic CAGE device and annulus, the configuration was similar, with the low-quality mesh (element size 3 mm, number of elements 4742, number of nodes 1817), medium-quality mesh (element size 1 mm, number of elements 19183, number of nodes 5113) and high-quality mesh (element size 0.5 mm, number of elements 115406, number of nodes 25518), each with its specific element size, number of elements and nodes. These settings were applied to perform a mesh convergence analysis. These settings were

Table 2
Mechanical properties of cortical and cancellous bone materials [36].

Bone	Density [g/cm^3]	Poisson ν	Young's Modulus E [MPa]
Cortical	1.8	0.3	12000
Cancellous	1.2	100	0.2
Posterior structure	1.8	0.25	3500

Table 3
Annulus modelled as hyperlastic Mooney-Rivlin solid.

C10	C01	G	K	Poisson ν
0.3448	0.3	1.288	644	0.499

Table 4
Mechanical and geometric characteristics of ligaments.

Ligaments	Total Area A_{tot} [mm^2]	N° Elements	Area used [mm2] A_u= A_{tot}/n° elements	Young's Modulus E [MPa]	Poisson ν
ALL	63.7	5	12.74	20	0.3
PLL	20	3	6.67	20	0.3
FL	40	3	13.33	19.5	0.3
ISL	40	4	10	11.5	0.3
SSL	30	3	10	15	0.3
CL	60	8	7.5	32.9	0.3

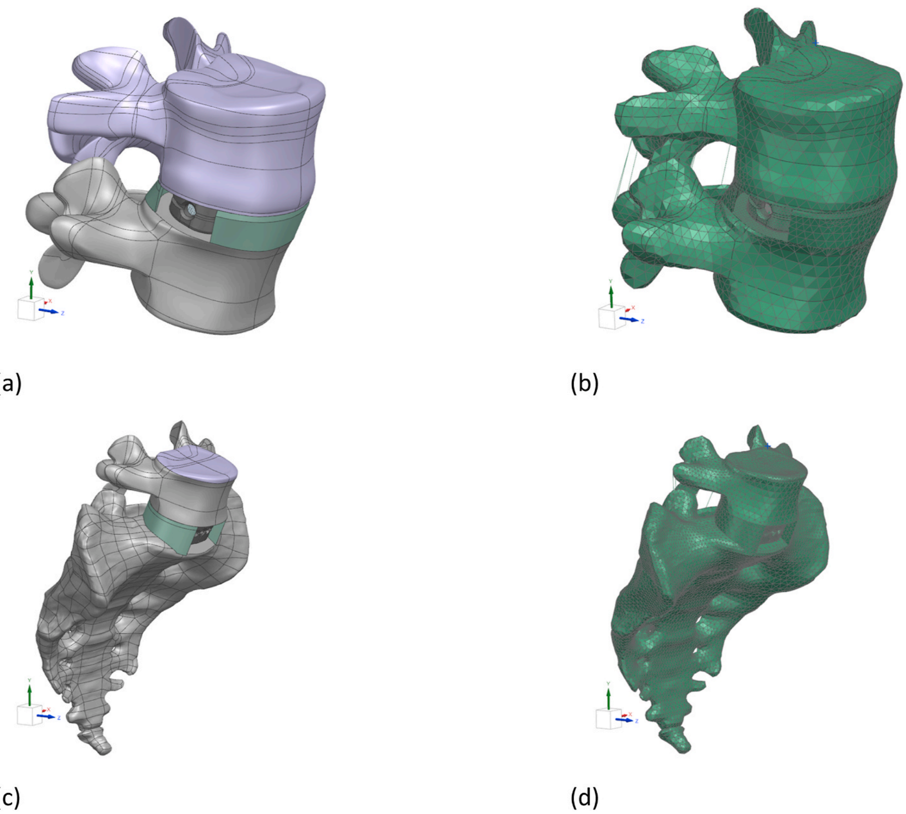

Fig. 6. The CAD models of L4-L5 (**a**) and L5-S1 (**c**) and the FEM model of L4-L5 (**b**) and L5-S1 (**d**).

applied to perform a mesh convergence analysis. To assess the sensitivity trend of the mesh, tables (show in Table 5 and Table 6) were generated highlighting variations in the maximum von Mises stress as the mesh size changed. An acceptability threshold was established, considering a variation of 5% in relation to the stress detected with the finest mesh used.

As a result of this convergence analysis, for the L4-L5 case, the chosen mesh setup was a tetrahedral mesh with 4 nodes, with

Table 5
The mesh sensitivity analysis for the vertebral pairs L4-L5 and L5-S1, highlighting variations in the maximum von Mises stress as mesh size changes.

L4-L5 and L5-S1	Size element 1 mm	Size element 3 mm	Size element 7 mm
The von Mises stress [MPa]	18.15	17.38	16.95
Diff %	–	4.24	6.63

Table 6
The mesh sensitivity analysis for the Intersomatic Cage and Annulus, highlighting variations in the maximum von Mises stress as mesh size changes.

Cage and annulus	Size element 0.5 mm	Size element 1 mm	Size element 3 mm
The von Mises stress	120.83	118.75	114.63
Diff %	–	1.72	5.13

dimensions of 3 mm on the vertebrae and 1 mm on the arthroprosthetic devices and the annulus. These same parameters were then applied to the L5-S1 case. The NET structure was modelled as beam elements, as regards the ligaments they were modelled with CROD elements. These types of modeling allows to decrease the number of element of the mesh and so increase the velocity of the simulation.

The boundary and load conditions of the two models were applied according to the study conducted by A. Shirazi et al. [42] carried out on the lumbar spine taken on cadavers. In this study, the authors have applied the concept of following the natural curvature of the lumbar spine (called 'following load'). The authors were able to apply compressive loads up to over 1000 N without any sign of instability. In cases A and B, the lower surface of the L5 vertebra was constrained as a fixed support, while on the upper surface of L4,

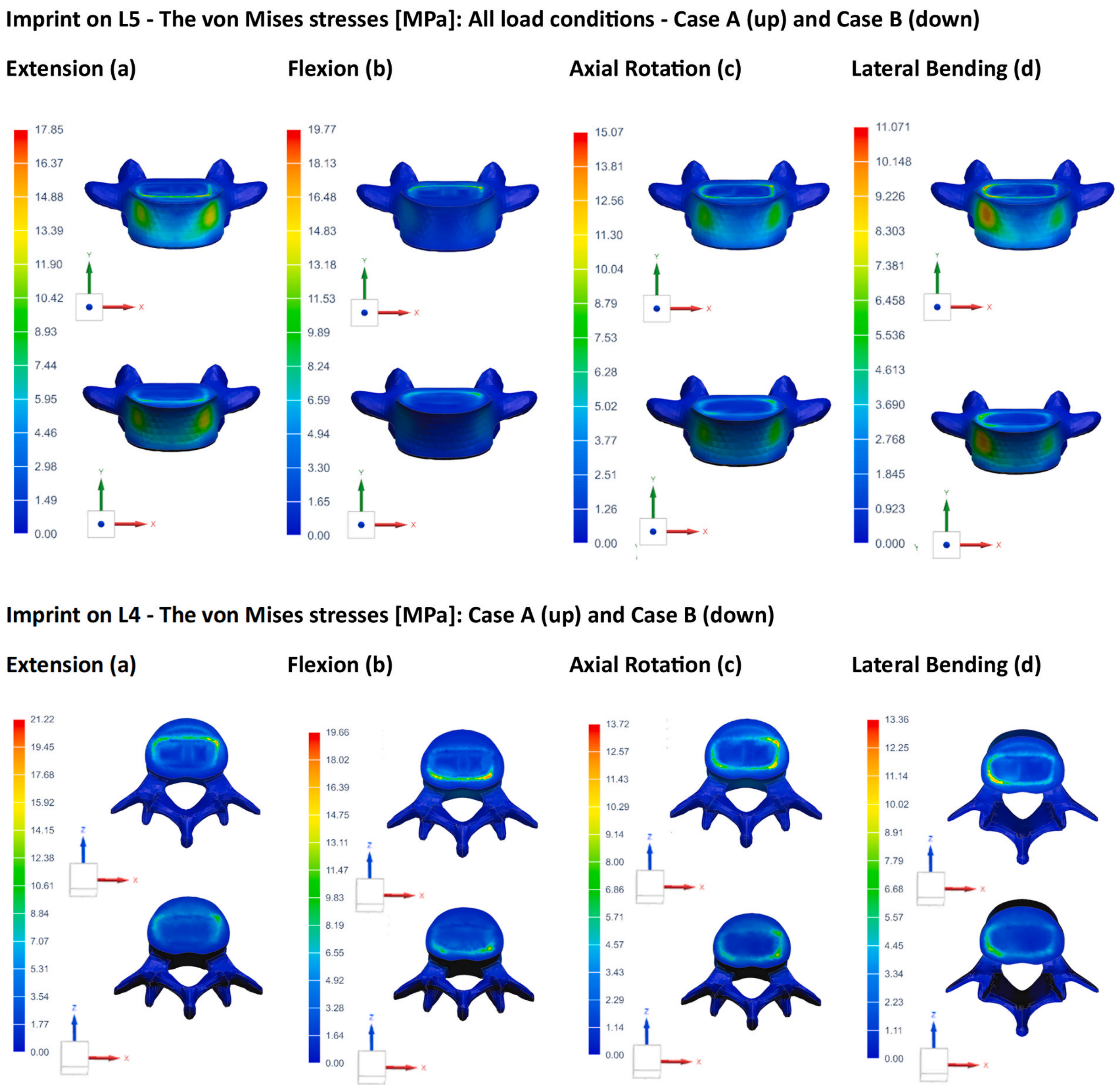

Fig. 7. Footprint distribution on the L4 and L5 vertebra under different loading conditions, for Case A and Case B. The movements considered include extension (**a**), flexion (**b**), axial rotation (**c**) and lateral flexion (**d**).

the load was applied through the use of a remote point connected to the surface of vertebra. In cases C and D, the S1 bone (sacrum) was constrained as a fixed support and the remote point was applied on the upper surface of L5. The contacts between the cages and the bone surfaces were considered as 'bonded' in order to emulate an osseointegration condition. Four loading conditions were simulated, which involved a compressive force of a maximum value of 1000 N, to which was added, individually, a rotational load.

1. pure bending moment of 7.5 Nm
2 .pure moment of extension equal to 7.5 Nm
3 .pure moment of axial torsion equal to 7.5 Nm
4. pure moment of lateral bending equal to 7.5 Nm.

Given the symmetry, the moments of torsion and lateral bending lead to equal and specular results when changed in sign.

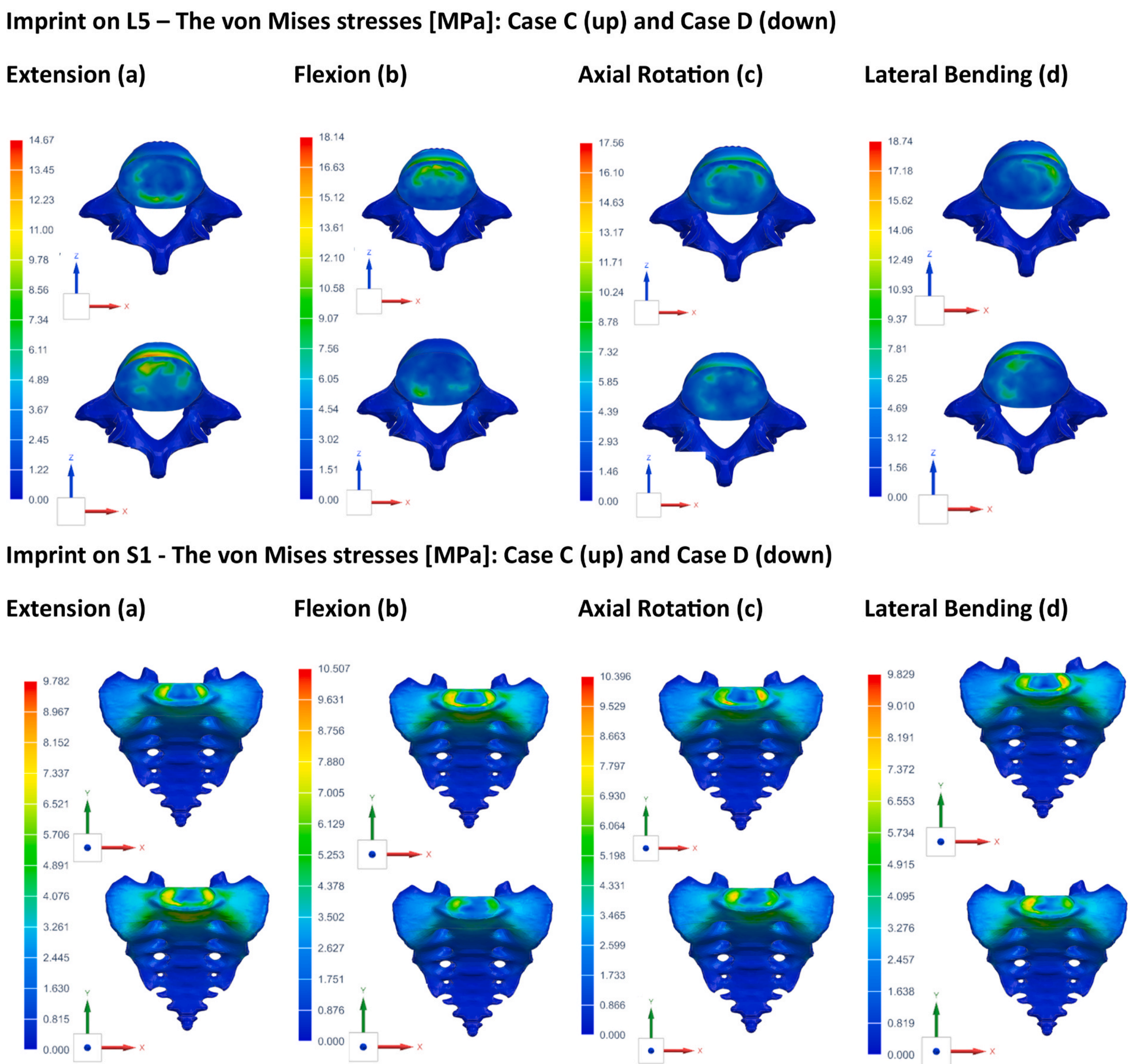

Fig. 8. Footprint distribution on the L5 and S1 vertebra under different loading conditions, for Case C and Case D. The movements considered include extension (**a**), flexion (**b**), axial rotation (**c**) and lateral flexion (**d**).

3. Results

3.1. Simulation FEM

Fig. 7 shows the stress values for all simulated boundary loads in the L4-L5 vertebrae, detailing the stress distribution for each vertebra in scenarios with and without a net for the four simulated load conditions. This includes the footprint distribution on the L4 and L5 vertebra under different loading conditions for Case A and Case B, with movements considered encompassing extension (Fig. 7a), flexion (Fig. 7b), axial rotation (Fig. 7c), and lateral flexion (Fig. 7d). The images enable us to observe the stress distribution arising from the insertion of the cage in terms of its impression and its redistribution across the entire vertebra. A direct comparison can be conducted between the two configurations under all simulated load conditions, highlighting differences in stress distribution and peak values.

Fig. 8 shows the stress values for all the boundary loads simulated on the L5 vertebra and S1 segment, also reporting the stress distribution for both cases is reported. This includes the footprint distribution on the L5 and S1 vertebra under different loading conditions for Case C and Case D, with movements considered encompassing extension (Fig. 8a), flexion (Fig. 8b), axial rotation (Fig. 8c), and lateral flexion (Fig. 8d).

In Table 7 and Table 8, the maximum von Mises stresses for all study cases and load conditions are reported highlighting differences among the simulated cases in terms of variations in peak stress values.

In Figs. 9 and 10, the distributions of von Mises stress across the anatomical features of interest are depicted. The images focus on the extension load condition for clarity, though this trend is consistent across all simulated load conditions, indicating a uniform pattern in the outcomes. Fig. 9 shows the stress distribution on the upper surface of the vertebrae L4-L5 for CASE A (Fig. 9a) and CASE B (Fig. 9b) under the extension load condition. Fig. 10 displays the stress distribution on the upper surface of the vertebrae L5-S1 for CASE C (Fig. 10a) and CASE D (Fig. 10b) under the same load condition.

3.2. Ligament reaction force and strain

In Table 9, the comparison of Cases A and B illustrates the varied impact of the Net structure on the reaction force of different ligaments within the intersomatic cage.

From the information in Table 10, detailing the percentage difference in strain between the cage with and without the Net structure (Case B compared to Case A).

Table 11 shows the results of the reaction forces of the ligaments in the L5-S1 vertebra couple.

Table 12, shows the percentage difference in strain between the cage with and without the Net structure in the case of the L5-S1 segment (Case D compared to Case C).

3.3. Range of motion

The Range of Motion (ROM) is a crucial aspect of spinal biomechanics, representing the relative range of motion between various pairs of vertebrae, in our case study these are L4-L5 and L5-S1 (Table 13).

3.4. Experimental validation

The simulations demonstrated that the introduction of intersomatic cages with a NET structure (cases B and D) reduced von Mises stresses compared to traditional cages (cases A and C) on the vertebral surfaces of L4, L5, and the S1 sacral tract. Specifically, stress distribution was more homogeneous, suggesting a potential improvement in load distribution. However, an exception was noted during the extension load for the L5-S1 segment, where the insertion of the NET structure led to an increase in stresses. These findings have direct implications for the design of cages, aiming to maximise osteointegration and minimise the risk of damage or premature

Table 7
The comparison of the maximum stresses in cases A and B, for all load conditions.

	CASE A	CASE B		
Extension	The von Mises stresses [MPa]		DIFF [MPa]	VAR %
L4	21.22	11.69	−9.5	−44.9
L5	17.85	12.82	−5.0	−28.2
Flexion	The von Mises stresses [MPa]		DIFF [MPa]	VAR %
L4	19.66	14.2	−5.5	−27.8
L5	19.77	10.59	−9.2	−46.4
Axial Rotation	The von Mises stresses [MPa]		DIFF [MPa]	VAR %
L4	13.72	10.18	−3.5	−25.8
L5	15.27	8.57	−6.5	−43.1
Lateral Bending	The von Mises stresses [MPa]		DIFF [MPa]	VAR %
L4	13.36	9.42	−0.39	−29.5
L5	11.07	9.58	−1.5	−13.4

Table 8
The comparison of the maximum stresses in cases C and D, for all load conditions.

	CASE C	CASE D		
Extension	The von Mises stresses [MPa]		DIFF [MPa]	VAR %
S1	7.94	9.78	1.8	23.2
L5	14.67	13.9	−0.8	−5.2
Flexion	The von Mises stresses [MPa]		DIFF [MPa]	VAR %
S1	10.5	7.46	−3.0	−29.0
L5	18.17	11.006	−7.2	−39.4
Axial Rotation	The von Mises stresses [MPa]		DIFF [MPa]	VAR %
S1	10.36	9.01	−1.4	−13.0
L5	17.59	9.94	−7.6	−43.5
Lateral Bending	The von Mises stresses [MPa]		DIFF [MPa]	VAR %
S1	9.82	9.34	−0.5	−5.0
L5	18.74	11.53	−7.2	−38.8

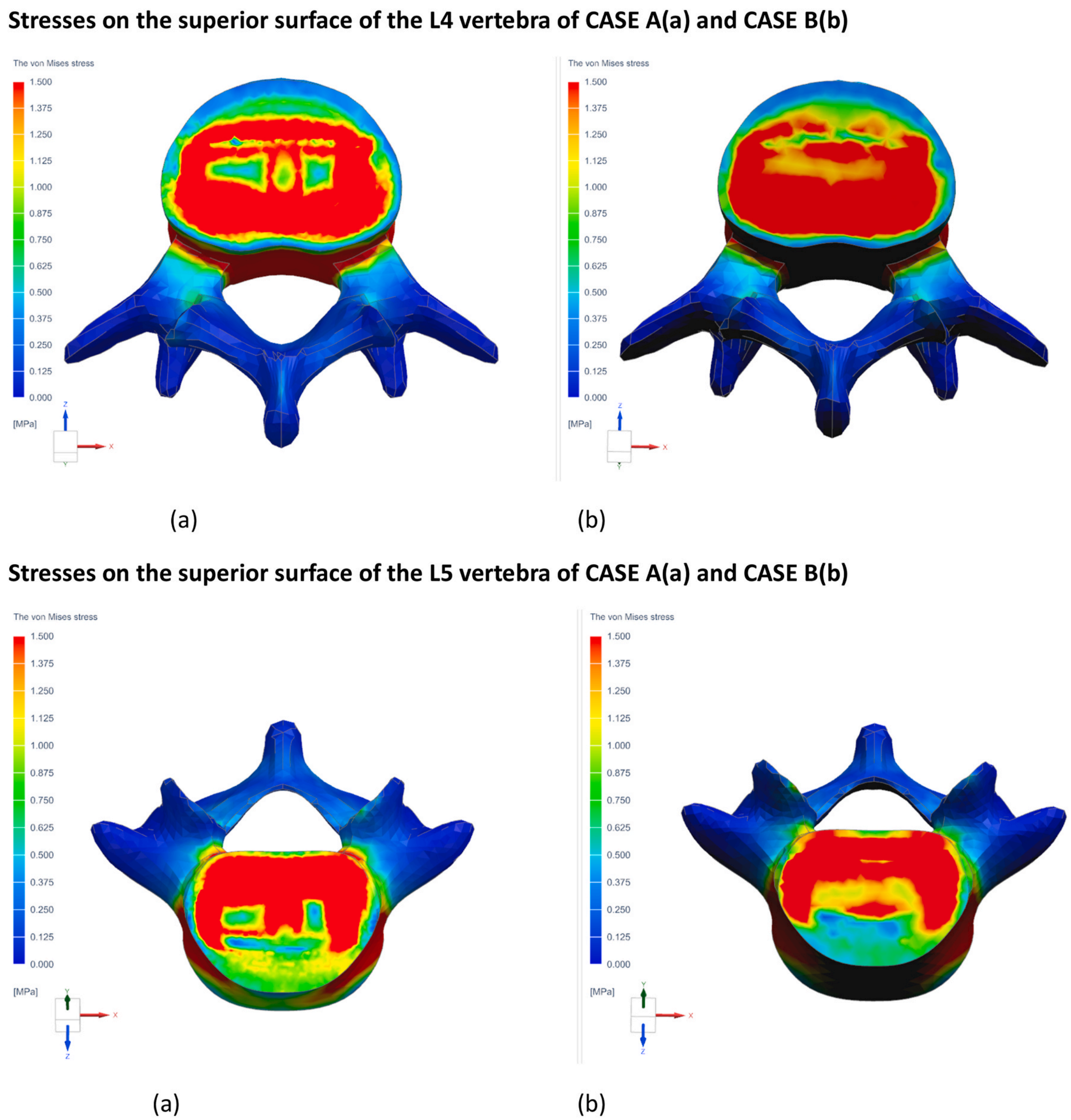

Fig. 9. The distribution of stress on the upper surface of the vertebrae for CASE A – CASE B in extension load condition.

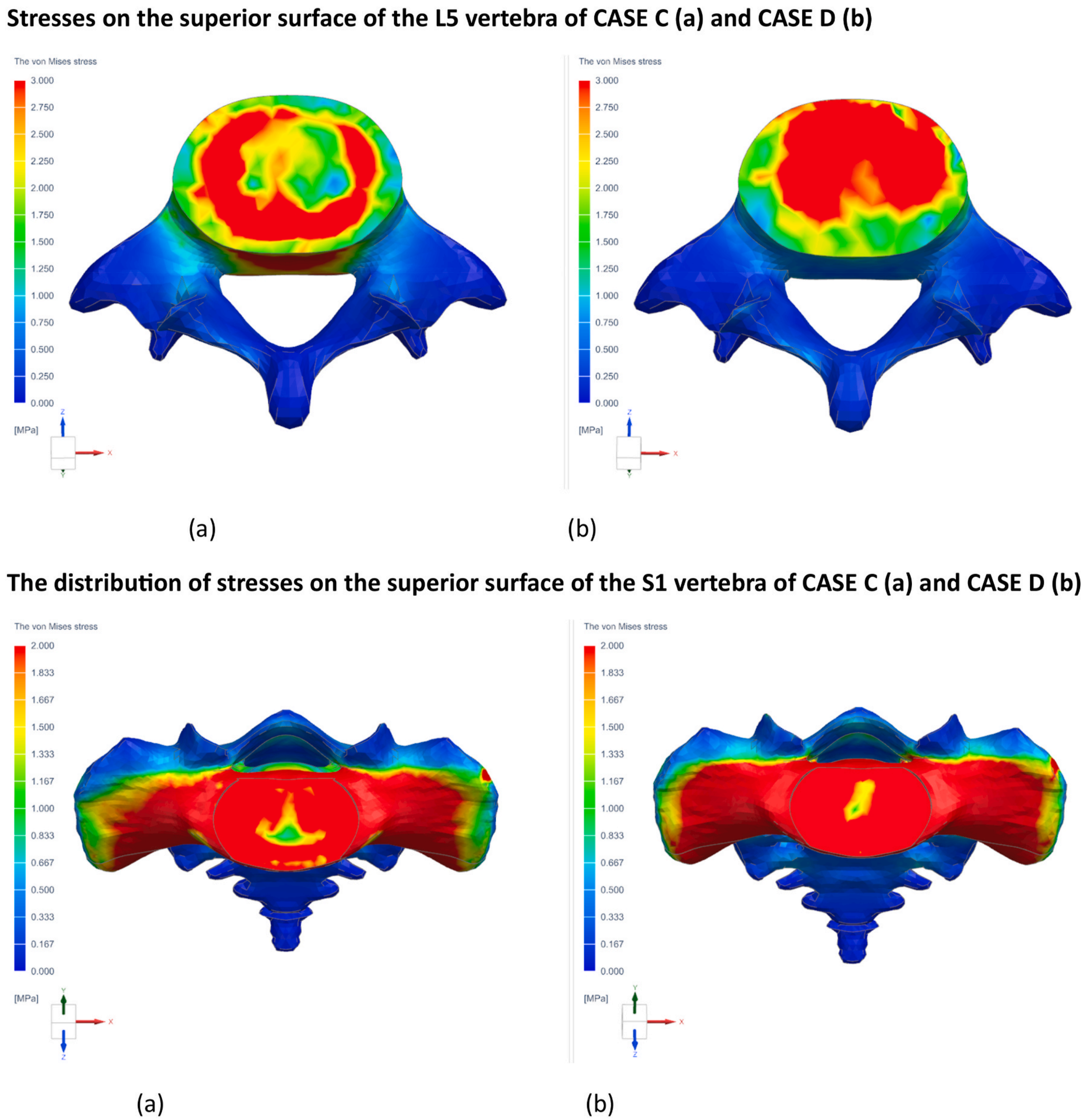

Fig. 10. The distribution of stress on the upper surface of the vertebrae L5-S1 for CASE C (a) – CASE D (b) in extension load condition.

Table 9
Comparison of cases A and B of ligament reaction force.

Difference between cage with net (Case B) vs cage without net (Case A) [%]				
Ligaments	Axial Rotation	Lateral Bending	Flexion	Extension
ALL	−1%	−30%	31%	−31%
PLL	20%	6%	26%	−31%
CL sx	18%	24%	11%	20%
CL dx	−3%	19%	1%	18%
FL	−11%	−163%	−22%	−28%
ISL	−6%	22%	−112%	30%
SSL	1%	26%	3%	18%

Table 10
Comparison of cases A and B of ligament strain.

Difference between cage with net (Case B) vs cage without net (Case A) [%]				
Ligaments	Axial Rotation	Lateral Bending	Flexion	Extension
ALL	24.0%	13.8%	15.2%	23.1%
PLL	91.2%	93.2%	92.4%	94.4%
CL sx	−22.0%	16.6%	−28.0%	32.2%
CL dx	−24.8%	−52.1%	22.6%	−22.3%
FL	−1.12%	−1.17%	8.33%	8.28%
ISL	−11.7%	−3.4%	−21.8%	−18.3%
SSL	−30.1%	−12.3%	−39.2%	−34.3%

Table 11
Comparison of cases C and D of ligament reaction force.

Difference between cage with net (Case D) vs cage without net (Case C) [%]				
Ligaments	Axial Rotation	Lateral Bending	Flexion	Extension
ALL	–	–	–	–
PLL	32%	21%	65%	49%
CL sx	−25%	−1%	70%	−17%
CL dx	25%	13%	34%	−26%
FL	−4%	34%	−34%	−145%
ISL	–	–	–	–
SSL	2%	−4%	12%	−7%

Table 12
Comparison of cases C and D of ligament strain.

Difference between cage with net (Case D) vs cage without net (Case C) [%]				
Ligaments	Axial Rotation	Lateral Bending	Flexion	Extension
ALL	–	–	–	–
PLL	11%	16%	1%	15%
CL sx	80%	79%	26%	63%
CL dx	−25%	−68%	25%	−38%
FL	29%	31%	49%	−28%
ISL	–	–	–	–
SSL	−2%	6%	48%	−54%

Table 13
Range of motion variation in the pairs of vertebrae L4-L5 and L5-S1.

Difference in Range of Motion (ROM) between cage with Net (Case B and D) vs cage without Net (Case A and C) [%]			
With Net vs Without Net	Axial Rotation	Lateral Bending	Flexion- Extension
CASE B VS CASE A	0.52%	−0.45%	0.14 %
CASE D VS CASE C	2.50%	24.60%	8.24 %

wear. In parallel, the analysis of ligament reaction force and deformability revealed that the introduction of the NET structure produces variable effects, in some cases relieving the load on ligaments, while in others it may exacerbate stress. Finally, the range of motion (ROM) study highlighted that, although variations for the L4-L5 segment were minimal, the L5-S1 segment exhibited significant increases, particularly in lateral flexion and extension-flexion, following the insertion of the NET structure. These results suggest that the introduction of a cage with a NET structure can have a considerable impact on ROM, particularly for the L5-S1 segment, an important consideration for clinical practice.

In comparing the data with the work of Chong Nan et al. [43], the analysis of the von Mises stress values for various biomechanical movements and vertebral levels demonstrates a similar general trend across the cases examined. This consistency in the stress patterns lends solid scientific validity to the study under review, as it indicates that the measurements of von Mises stress can be considered reliable and reproducible in different experimental contexts. The data comparison (show in Fig. 11) reveals that, although there are some differences in the absolute stress values between CASE A and CASE B and the study by Chong Nan et al., the relative trend remains consistent. For instance, in conditions of extension and flexion, CASE A tends to exhibit higher values compared to CASE B, but aligns with the findings reported by Chong Nan et al. in terms of which vertebral level is more stressed. This similarity suggests that the biomechanical factors contributing to vertebral stress have been modelled similarly across various studies, despite potential

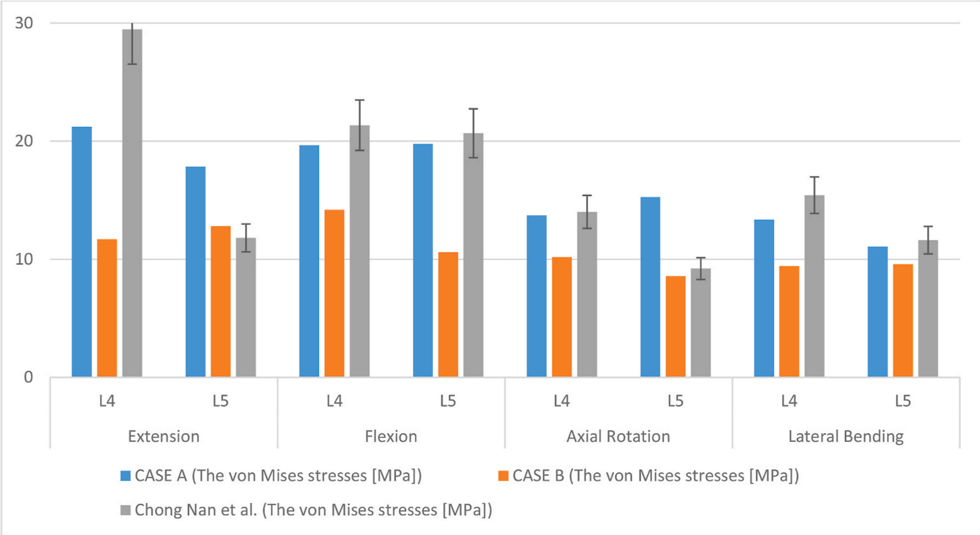

Fig. 11. The comparison between cases with net, without net and in the literature.

methodological differences.

Furthermore, the detailed analysis of the data provides additional insights. The higher stress values observed in CASE A might suggest a potentially increased risk of material failure or damage to vertebral structures. However, the fact that these values are in line with those reported by Chong Nan et al. suggests that such risks are inherent to the biomechanics of spinal fusion and not necessarily an artefact of a particular experimental or clinical design. The differences between vertebral levels, such as the increased stress observed at the L5 level under certain movement conditions, reflect the biomechanical reality that lower levels of the spine are typically subjected to greater loads. This parallelism between the experimental data and the underlying biomechanical understanding strengthens the validity of the study's results. The clinical implications of these data are significant. The confirmation that the implant designs and surgical techniques used in the study produce a stress trend corresponding to that observed in other scientific works supports the reliability of the approaches used. This consistency across studies is vital for building a body of knowledge that can guide clinical decisions and the design of future implants. Finally, it is important to acknowledge that, although von Mises stress data provide a measure of mechanical load distribution, comprehensive clinical analysis requires a multifactorial evaluation that includes long-term patient outcomes, the prevalence of complications, and post-intervention quality of life. Therefore, biomechanical data should always be integrated with clinical data to provide the best recommendations for clinical practice.

4. Discussion

4.1. Simulation FEM

The analysis of von Mises stresses and their distribution across the anatomical elements studied—specifically, the L4 and L5 vertebrae and the S1 sacral segment—alongside the stresses on the intervertebral arthroprosthetic devices, reveals significant findings. The data indicate that the reengineered cages in cases B and D, which incorporate a Net structure, exhibit lower stresses on the vertebrae and the S1 sacral tract compared to the cages without a net in cases A and C. Fig. 7 details the stress values for all boundary loads simulated on the L4-L5 vertebrae, presenting stress distribution for each vertebra in both the presence and absence of the net across four simulated load conditions. It is observed that the stress distribution for the cage with the Net is lower, with the maximum stress peaks occurring in cases A and C, where the cage lacks a Net structure.

Fig. 8 further illustrates the stress values for all boundary loads simulated on the L5 vertebra and the S1 tract, reporting the stress distribution in both scenarios. Here too, an overall improvement in cage behavior is noted, with an exception for the extension load condition on the L5 and S1 tract. Under this specific load condition, the insertion of the Net into the cage may lead to an increase in stresses within the involved bone structures.

Tables 7 and 8 compile the maximum von Mises stresses for all study cases and load conditions, comparing cages with and without the Net. Negative variations in this comparison indicate a reduction in stresses for cages equipped with the reticular structure. However, the analysis highlights an increase in stress on the L5-S1 tract during the extension load as the only condition adversely affected by the insertion of the Net within the cage.

Overall, the von Mises stress distributions on the interior surfaces of L4 and the superior surfaces of L5, as well as the inferior surfaces of L5 and the superior surfaces of S1, demonstrate a more homogeneous distribution with the use of NET-structured cages. This homogeneity effectively spreads the load across the entire surface, resulting in improved load distribution compared to cages lacking the Net structure, as depicted in Figs. 9 and 10. The images, focusing on the extension load condition for brevity but applicable to all simulated load conditions, showcase a very homogenous stress distribution in cases B and D, leading to an optimal load distribution.

4.2. Ligament reaction force and strain

The results concerning the ligaments' reaction forces and strain highlight that the introduction of the Net structure manifests both advantageous and detrimental effects, varying by the specific ligament and the movement type. These insights are pivotal for guiding the design and implementation of interbody cages. Further investigation is essential to fully elucidate the functional and clinical implications of these observations.

The results presented in Table 9 illustrate the diverse impacts of incorporating the Net structure within the interbody cage on various ligaments' reaction forces. These findings indicate that there is no significant disparity in the behavior of the two types of cages. Depending on the loading conditions, the Net can either alleviate the load on some ligaments or exacerbate stress on others. The Anterior Longitudinal Ligament (ALL) demonstrates a decrease of 1% in axial rotation and 30% in lateral bending with the introduction of the Net, and an increase of 31% in flexion, and a decrease of 31% in extension. This indicates that the Net structure might lessen the reaction force of the ALL during axial rotation and lateral bending, but increase it during flexion and reduce it during extension. The Posterior Longitudinal Ligament (PLL) shows an increase of 20% in axial rotation and 6% in lateral bending, an increase of 26% in flexion, and a decrease of 31% in extension with the Net. This suggests that the Net might enhance the reaction force of the PLL during axial rotation and lateral bending, but increase it during flexion and reduce it during extension. The capsular ligaments (CL) show an increase in reaction force with the introduction of the Net, indicating that the Net might enhance the reaction force of the CL. Conversely, the flavum ligament (FL) shows a significant reduction in reaction force in all directions with the Net, suggesting that the Net might decrease the reaction force of the FL. The interspinous ligament (ISL) presents a decrease in reaction force in axial rotation and flexion, and an increase in lateral bending and extension with the Net. This suggests that the Net might decrease the reaction force of the ISL during axial rotation and flexion, but increase it during lateral bending and extension. Finally, the supraspinous ligament (SSL) shows a general increase in reaction force with the Net, suggesting that the Net might enhance the reaction force of the SSL. In general, the introduction of the Net can lead to both increases and decreases in the reaction force of ligaments, depending on the specific ligament and the type of movement considered. These results can guide the design and use of intersomatic cages with Net structures. However, further research might be necessary to better understand the functional and clinical implications of these changes.

Following the data presented in Table 10, the subsequent observations can be highlighted. The Anterior Longitudinal Ligament (ALL) shows an increase in strain across all movements with the introduction of the Net. The Posterior Longitudinal Ligament (PLL) presents a considerable increase in strain across all movements. The capsular ligaments (CL) show a variation in strain with the introduction of the Net. Specifically, the left capsular ligament (CL sx) shows a decrease in strain during axial rotation and flexion, but an increase in lateral bending and extension. The right capsular ligament (CL dx) exhibits a decrease in strain during axial rotation and lateral bending, but an increase in flexion and a decrease in extension. The flavum ligament (FL) shows a slight decrease in strain during axial rotation and lateral bending, but an increase in flexion and extension. The interspinous ligament (ISL) presents a decrease in strain across all movements with the introduction of the Net. Finally, the supraspinous ligament (SSL) shows a general decrease in strain with the introduction of the Net.

From Tables 11 and it is evident that the Anterior Longitudinal Ligament (ALL) is absent in this case. This absence is due to the anterior insertion of the cage, necessitating the removal of the ALL to accommodate the cage within the interbody space of the L5-S1 vertebrae pair. As outlined in the study by Roberto Bassani et al., this removal is part of the Anterior Lumbar Interbody Fusion (ALIF) procedure, which involves a partial resection of the ALL to facilitate the placement of the intersomatic device [44]. The interspinous ligament (ISL) was not considered, possibly due to its minor importance in the L5-S1 segment for anatomical or biomechanical reasons.

The Posterior Longitudinal Ligament (PLL) shows an increase in reaction forces across all movements with the introduction of the Net, with the most substantial increase in flexion (65%) followed by extension (49%), axial rotation (32%), and lateral bending (21%). This suggests that the Net may enhance the PLL's load-bearing capacity across all these movements.

The reaction forces of the capsular ligaments (CL) appear to vary for the left and right sides with the introduction of the Net. The left capsular ligament (CL sx) shows a decrease in axial rotation and extension (25% and 17% respectively), a slight decrease in lateral bending (1%), but a significant increase in flexion (70%). The right capsular ligament (CL dx) presents an increase in axial rotation, lateral bending, and flexion (25%, 13%, and 34% respectively), but a decrease in extension (26%). This suggests that the Net might differently affect the left and right capsular ligaments' load-bearing capacity.

The flavum ligament (FL) shows a slight decrease in axial rotation (4%), a substantial decrease in extension (145%), but an increase in lateral bending (34%) and a decrease in flexion (34%) with the Net. This indicates that the Net might decrease the FL's load-bearing capacity during axial rotation, extension, and flexion, but increase it during lateral bending.

Finally, the supraspinous ligament (SSL) shows a minor increase in axial rotation and flexion (2% and 12% respectively), a minor decrease in lateral bending and extension (4% and 7% respectively) with the Net. This suggests that the Net may slightly affect the SSL's load-bearing capacity across all these movements.

From Tables 12 and it can be observed how the Posterior Longitudinal Ligament (PLL) shows a slight increase in strain across all movements with the introduction of the Net. The capsular ligaments (CL) display a variation in strain with the introduction of the Net. Specifically, the left capsular ligament (CL sx) shows a considerable increase in strain across all movements, while the right capsular ligament (CL dx) exhibits a decrease in strain during axial rotation and lateral bending, but an increase in flexion and a decrease in extension. The flavum ligament (FL) demonstrates an increase in strain during axial rotation, lateral bending and flexion, but a decrease in extension with the introduction of the Net. The interspinous ligament (ISL) has not been considered in this case. Lastly, the supraspinous ligament (SSL) shows a minor decrease in strain during axial rotation, an increase in lateral bending and flexion, and a significant decrease in extension with the introduction of the Net.

4.3. Range of motion

In the context of spinal biomechanics research, the Range of Motion (ROM) represents a critical aspect, defining the degree of relative movement between various pairs of vertebrae, in our specific case study the L4-L5 and L5-S1 pairs (Table 13). The introduction of the interbody cage between the vertebrae in place of the intervertebral disc nucleus pulposus can influence the degrees of freedom allowed by a specific joint, which can have significant clinical implications.

Regarding the comparison between Case B and Case A (Case B with Net vs Case A without Net), which presumably involves the L4-L5 vertebrae pair, the ROM changes are relatively minor when introducing the Net. There is a slight increase in axial rotation (0.52%) and flexion-extension (0.14%) with the Net, while there is a slight decrease (−0.45%) in lateral bending. For Case D vs Case C (Case D with Net vs Case C without Net), presumably involving the L5-S1 vertebrae pair, the ROM changes are more pronounced. There is an increase in all three types of movements. Axial rotation increases by 2.50%, which is a relatively modest change. However, the lateral bending and flexion-extension show more significant increases, 24.60% and 8.24% respectively. These results suggest that the introduction of the Net to the cage has a more substantial impact on ROM for the L5-S1 vertebrae pair than the L4-L5 pair. This could be due to the unique anatomical and biomechanical characteristics of the L5-S1 segment, which is often subject to greater stresses and movements compared to other parts of the spine.

The significant differences observed in lateral bending (24.60%) and flexion-extension (8.24%) for Case D vs Case C, which represents the L5-S1 vertebrae pair, could indeed be due to the absence of the Anterior Longitudinal Ligament (ALL). The ALL provides substantial stability to the spinal column, particularly in restricting excessive extension movements. Without the stabilizing influence of the ALL in the L5-S1 segment, the introduction of the Net to the cage could have a more pronounced effect on spinal movement. In particular, it may allow for greater freedom in lateral bending and flexion-extension, hence the noticeable increase in the ROM for these movements. Clinically, the absence of the ALL in the L5-S1 segment is compensated by other ligaments and especially muscle structures that were not considered in this study. Therefore, the simulation can be improved, e.g. by including the muscular apparatus. The inclusion of muscle forces would provide a more accurate representation of the biomechanical environment of the spinal segment and may help to better understand the functional and clinical implications of introducing a cage with a Net structure in different vertebral segments. Further research in this direction would be highly beneficial.

4.4. Comparison in the literature and limitations of the study

In the literature, there are numerous studies providing valuable insights into lumbar interbody fusion techniques and the management of pubic symphysis diastasis through various fixation methods, highlighting the evolution towards less invasive and more effective approaches. Lumbar interbody fusion, as demonstrated by Qin et al. [45], underscores the significance of the interbody cage's position in minimizing stress and reducing the risk of postoperative complications, such as cage subsidence. Cai et al. [46], through biomechanical analysis, reveal how different internal fixation devices impact postoperative stability, suggesting that the addition of lateral plates could significantly enhance stability. Zheng et al. [47] explore the biomechanics of seven fixation methods for pubic symphysis diastasis, revealing that specific devices, like cannulated cross screws, provide optimal results in terms of stability and stress resistance, indicating a potential refinement of current surgical strategies.

The work by Ji et al. [48] represents a notable contribution to the field of spinal biomechanics, focusing on the biomechanical characteristics of two posterior fixation methods with bilateral pedicle screws through finite element analysis. This study shows that pedicle screw fixation in two vertebrae called model A (L3 and L5) can achieve similar stability to fixation in three vertebrae called model B (L3, L4, L5), but with less stress on the fixation system components in model B, suggesting a reduced risk of fracture. The detailed methodology and analytical approach adopted by the authors highlight the importance of finite element analysis as a tool for optimising surgical treatment strategies of the spine, providing a solid foundation for further research and development in the field of spinal biomechanics. In addition to the great importance of the use of finite element methods, the study by Ji et al. also highlighted a significant limitation of studies employing numerical simulations to describe human biological functions, which are influenced by patients' clinical histories, including conditions such as osteoporosis and other diseases. Of course, these kinds of limitations are also present in our research, despite the use of different prostheses: intervertebral cages for this study, versus the pedicle screws used in Ji et al.'s study. There remain some shortcomings in the application of this model, for example, the friction coefficient between surfaces might not accurately reflect the actual situation. Moreover, exogenous stability factors of the spine, such as muscles, are overlooked, and there is a simplification of some structures, like ligaments treated in a one-dimensional manner. Real degenerative conditions such as bone loss or ligament relaxation are not considered, and the material parameters used are standard values, which could lead to specific results differing from reality which can be influenced by the orthopedic condition of each individual patient.

Even the study conducted by Song et al. [49] and Cen et al. [50] highlight the potential limitations of approaches based on finite element methods. Although these studies focus on understanding foot biomechanics, the generic limitations explained in these papers are applicable to our studies. Interestingly, the limitations identified in these studies, such as the use of a single subject, mirror the same concerns in the present work, highlighting how such an approach can raise questions about the generalizability of the findings. This limitation underscores the importance of considering individual patient response to these kinds of variations in foot biomechanics and the need for future research that includes larger samples to confirm and expand upon the current findings. Despite these limitations, the simulations provide an accurate general representation under the same experimental conditions, with the advantages of low simulation costs, no risk to patients, and convincing results, thus making a significant contribution to clinical practice. The complex biomechanics of the human body are influenced by numerous factors, reflecting the intricate interplay between structure and function. Future studies that aim to examine the entire spine and include the lower limbs could offer profound insights into human locomotion. By integrating comprehensive models of the spine with the mechanics of lower limbs, researchers could evaluate how different components interact during walking. This holistic approach would not only enhance our understanding of the body's biomechanical behavior but also inform more effective treatments and interventions for mobility-related issues.

5. Conclusion

The study intends to take advantage of a computer-aided engineering (CAE) method to evaluate the efficiency of different cage solutions. Employing CAE methods can offer a more accurate and detailed evaluation of the performance of various devices, especially when considering intricate factors like the inclusion of NET. Thanks to a CAE approach it is possible to evaluate several aspects of these kind of implants in terms of von Mises stresses, pressure distribution on cage and Range of Motion of the patient. The primary objective of the study discussed in the article is to verify and compare the level of von Mises stress on the bone surface of the vertebrae when different types of arthroprosthetic devices are inserted, specifically comparing cages with and without the NET. This comparison is pivotal in understanding how the presence or absence of NET might influence the stress distribution on the vertebrae, and consequently, their long-term functionality and integrity. Drawing upon the insights from Polikeit et al. (2003) [51] understanding the interaction between the endplate and the interbody cages is crucial for optimising spinal fusion outcomes. By assessing the level of stress in different positions of the vertebrae, the study allows for the identification of the maximum stress value, its distribution, and its position. This is crucial for a clear understanding of how and where stress is allocated, potentially assisting in designing more efficient and safer devices. Additionally, an investigation into the Range of Motion (ROM) has been undertaken. This provides vital insights into how these devices, with or without NET, might affect the flexibility and movement capabilities of the spine. Another important aspect is the assessment of pressure distribution on the cage, the pressure must be optimally distributed in order to reduce associated risks of damage and premature wear. If an implant, with or without NET, produces a distribution of pressure inadequate or to unintended areas, it could result in premature wear, instability, or even failure of the implant or surrounding bone tissue. Understanding how arthroprosthetic implants, particularly cages with and without NET, affect bone structures is crucial. Discopathies can cause significant discomfort and limit daily activities. While arthroprosthetic implants aim to alleviate pain and enhance mobility, it's vital to ensure they don't inadvertently cause further complications. The inclusion of the Range of Motion study further clarifies the potential effects of these implants on the overall movement and function of the spinal region.

In conclusion, the study presented in the article focuses on the effects of arthroprosthetic implants on bone structure in cases of discopathy, with particular attention to the lumbosacral tract of the spinal column. The main goal of the paper is to reengineering a traditional cage exploiting additive manufacturing technology and so the possibility of manufacturing complex geometries. The analysis is based on static FEA simulations of two clinical cases involving the L4-L5 and L5-S1 intervertebral discs, using two types of cages: LLIF for L4-L5 and ALIF for L5-S1. Each model was tested with four different loading conditions obtained by applying a compression load of 1000 N plus a 7.5 Nm moment applied individually for extension, flexion, torsion, and lateral bending rotations.

The results show that the stresses exerted by the cages with a NET structure (cases B and D) are generally lower than those of the cages without a net (cases A and C), indicating a more concentrated load distribution and a lower contact surface, leading to suffering and in some cases possible failure of the bone structure, losing intervertebral height. The negative variations in Tables 7 and 8 indicate a reduction in stresses in the cages equipped with a NET lattice structure compared to those without.

In summary, the work carried out in this article suggests that the use of intervertebral cages with a NET internal lattice structure may lead to a reduction in stresses on the vertebrae and an improvement in load distribution, which could have positive implications for osseointegration and spinal stability. However, further research and clinical studies are needed to confirm the findings and assess the effectiveness of these cages in clinical practice and further analysis are needed to improve the CAE approach used introducing also muscles.

Data availability statement

The raw data supporting the conclusion of this article will be made available on request.

CRediT authorship contribution statement

Filippo Cucinotta: Writing – review & editing, Validation, Conceptualization. **Rosalia Mineo:** Visualization, Conceptualization. **Marcello Raffaele:** Writing – review & editing, Writing – original draft, Validation, Software, Methodology, Investigation, Data curation. **Fabio Salmeri:** Visualization, Resources, Data curation. **Fulvio Tartara:** Visualization, Conceptualization. **Felice Sfravara:** Writing – review & editing, Writing – original draft, Validation, Methodology, Formal analysis.

Declaration of competing interest

The authors declare that they have no known competing financial interests or personal relationships that could have appeared to influence the work reported in this paper.

Acknowledgement

This work has been supported by the project "GOALS, Green Optimizations by Additive-manufactured Lightweight Structures", Project 20228PFA89, CUP J53D23001980006, Progetti di Ricerca di Rilevante Interesse Nazionale PRIN 2022, funded under the National Recovery and Resilience Plan (NRRP), Mission 4 Component C2 Investment 1.1 by the European Union – NextGenerationEU.

References

[1] S. Saleem, H.M. Aslam, M.A. khan Rehmani, A. Raees, A.A. Alvi, J. Ashraf, Lumbar disc degenerative disease: disc degeneration symptoms and magnetic resonance image findings, Asian Spine J 7 (2013) 322.
[2] R. Roy-Camille, M. Roy-Camille, C. Demeulenaere, [Osteosynthesis of dorsal, lumbar, and lumbosacral spine with metallic plates screwed into vertebral pedicles and articular apophyses], Presse Med. 78 (1970) 1447–1448.
[3] L. Balabaud, E. Gallard, W. Skalli, B. Dupas, R. Roger, F. Lavaste, J.-P. Steib, Biomechanical evaluation of a bipedicular spinal fixation device: three different strength tests, Eur. Spine J. 12 (2003) 480–486.
[4] M.C. Whitbeck, Posterior cervical plate-screw fixation, Oper. Tech. Orthop. 8 (1998) 34–45.
[5] F. Distefano, S. Pasta, G. Epasto, Titanium lattice structures produced via additive manufacturing for a bone scaffold: a review, J. Funct. Biomater. 14 (2023) 125.
[6] E. Barberi, F. Cucinotta, M. Raffaele, F. Salmeri, A hollowing topology optimization method for additive and traditional manufacturing Technologies, in: Lect. Notes Mech. Eng., 2022.
[7] F. Cucinotta, M. Raffaele, F. Salmeri, A stress-based topology optimization method by a Voronoi tessellation Additive Manufacturing oriented, Int. J. Adv. Manuf. Technol. 103 (2019) 1965–1975.
[8] F. Cucinotta, M. Raffaele, F. Salmeri, A Topology Optimization of a Motorsport Safety Device, 2020, pp. 400–409.
[9] N. Kos, L. Gradisnik, T. Velnar, A brief review of the degenerative intervertebral disc disease, Med. Arch. 73 (2019) 421.
[10] T.L. Siu, J.M. Rogers, K. Lin, R. Thompson, M. Owbridge, Custom-made titanium 3-dimensional printed interbody cages for treatment of osteoporotic fracture–related spinal deformity, World Neurosurg 111 (2018) 1–5.
[11] S. Schleifenbaum, R. Heilmann, E. Riemer, R. Reise, C.-E. Heyde, J.-S. Jarvers, P. Pieroh, A. Völker, N.H. von der Hoeh, A biomechanical model for testing cage subsidence in spine specimens with osteopenia or osteoporosis under permanent maximum load, World Neurosurg 152 (2021) e540–e548.
[12] R. Lo Giudice, C. Galletti, J.P.M. Tribst, L.P. Melenchón, M. Matarese, A. Miniello, F. Cucinotta, F. Salmeri, In vivo analysis of intraoral scanner precision using open-source 3D software, Prosthesis 4 (2022) 554–563.
[13] F. Cucinotta, R. Mineo, M. Raffaele, F. Salmeri, F. Sfravara, Customized implant of cervical prostheses exploiting a predictive analysis of range of motion, Comput. Aided. Des. Appl. (2022) 122–133.
[14] G. Bagby, The Bagby and Kuslich (BAK) method of lumbar interbody fusion, Spine 24 (1999) 1857.
[15] L. Caliogna, V. Bina, L. Botta, F.M. Benazzo, M. Medetti, G. Maestretti, M. Mosconi, F. Cofano, F. Tartara, G. Gastaldi, Osteogenic potential of human adipose derived stem cells (hASCs) seeded on titanium trabecular spinal cages, Sci. Rep. 10 (2020) 18284.
[16] E. Ragni, C. Perucca Orfei, A. Bidossi, E. De Vecchi, N. Francaviglia, A. Romano, G. Maestretti, F. Tartara, L. de Girolamo, Superior osteo-inductive and osteo-conductive properties of trabecular titanium vs. PEEK scaffolds on human mesenchymal stem cells: a proof of concept for the use of fusion cages, Int. J. Mol. Sci. 22 (2021) 2379.
[17] F. Cucinotta, M. Raffaele, F. Salmeri, A Topology Optimization Method for Stochastic Lattice Structures (2021) 235–240.
[18] F. Cucinotta, R. Mineo, M. Raffaele, F. Salmeri, Assessment of the run-out of an intervertebral cervical cage fabricated by additive manufacturing using electron beam melting, in: Proc. ASME Des. Eng. Tech. Conf., 2021.
[19] S.J. Atlas, R.A. Deyo, Evaluating and managing acute low back pain in the primary care setting, J. Gen. Intern. Med. 16 (2001) 120–131.
[20] C.-S. Chen, C.-K. Cheng, C.-L. Liu, W.-H. Lo, Stress analysis of the disc adjacent to interbody fusion in lumbar spine, Med. Eng. Phys. 23 (2001) 485–493.
[21] F. Heuer, H. Schmidt, L. Claes, H.-J. Wilke, A new laser scanning technique for imaging intervertebral disc displacement and its application to modeling nucleotomy, Clin. Biomech. 23 (2008) 260–269.
[22] F. Heuer, H. Schmidt, Z. Klezl, L. Claes, H.-J. Wilke, Stepwise reduction of functional spinal structures increase range of motion and change lordosis angle, J. Biomech. 40 (2007) 271–280.
[23] H.-M. Lin, Y.-N. Pan, C.-L. Liu, L.-Y. Huang, C.-H. Huang, C.-S. Chen, Biomechanical comparison of the K-ROD and Dynesys dynamic spinal fixator systems – a finite element analysis, Bio Med. Mater. Eng. 23 (2013) 495–505.
[24] D.W. McMillan, D.S. McNally, G. Garbutt, M.A. Adams, Stress distributions inside intervertebral discs: the validity of experimental 'stress profilometry, Proc. Inst. Mech. Eng. Part H J. Eng. Med. 210 (1996) 81–87.
[25] A. Rohlmann, S. Neller, L. Claes, G. Bergmann, H.-J. Wilke, Influence of a follower load on intradiscal pressure and intersegmental rotation of the lumbar spine, Spine 26 (2001) E557–E561.
[26] H. Schmidt, M. Bashkuev, M. Dreischarf, A. Rohlmann, G. Duda, H.-J. Wilke, A. Shirazi-Adl, Computational biomechanics of a lumbar motion segment in pure and combined shear loads, J. Biomech. 46 (2013) 2513–2521.
[27] A.Y.L. Wong, G. Harada, R. Lee, S.D. Gandhi, A. Dziedzic, A. Espinoza-Orias, M. Parnianpour, P.K. Louie, B. Basques, H.S. An, D. Samartzis, Preoperative paraspinal neck muscle characteristics predict early onset adjacent segment degeneration in anterior cervical fusion patients: a machine-learning modeling analysis, J. Orthop. Res. 39 (2021) 1732–1744.
[28] I. Yamamoto, M.M. Panjabi, T. Crisco, T. Oxland, Three-dimensional movements of the whole lumbar spine and lumbosacral joint, Spine 14 (1989) 1256–1260.
[29] A. Faizan, A. Kiapour, A.M. Kiapour, V.K. Goel, Biomechanical analysis of various footprints of transforaminal lumbar interbody fusion devices, J. Spinal Disord. Tech. 27 (2014) E118–E127.
[30] V.K. Goel, A. Mehta, J. Jangra, A. Faizan, A. Kiapour, R.W. Hoy, A.R. Fauth, Anatomic facet replacement system (afrs) restoration of lumbar segment mechanics to intact: a finite element study and in vitro cadaver investigation, Int. J. Spine Surg. 1 (2007) 46–54.
[31] Y. Guan, N. Yoganandan, J. Moore, F.A. Pintar, J. Zhang, D.J. Maiman, P. Laud, Moment–rotation responses of the human lumbosacral spinal column, J. Biomech. 40 (2007) 1975–1980.
[32] A. Kiapour, D.G. Anderson, D.B. Spenciner, L. Ferrara, V.K. Goel, Kinematic effects of a pedicle-lengthening osteotomy for the treatment of lumbar spinal stenosis, J. Neurosurg. Spine 17 (2012) 314–320.
[33] A. Nachemson, Lumbar intradiscal pressure: experimental studies on post-mortem material, Acta Orthop. Scand. 31 (1960) 1–104.
[34] M.M. Panjabi, T.R. Oxland, I. Yamamoto, J.J. Crisco, Mechanical behavior of the human lumbar and lumbosacral spine as shown by three-dimensional load-displacement curves, J. Bone Jt. Surg. 76 (1994) 413–424.
[35] M.J. Pearcy, Stereo radiography of lumbar spine motion, Acta Orthop. Scand. 56 (1985) 1–45.
[36] Z.-C. Zhong, S.-H. Wei, J.-P. Wang, C.-K. Feng, C.-S. Chen, C. Yu, Finite element analysis of the lumbar spine with a new cage using a topology optimization method, Med. Eng. Phys. 28 (2006) 90–98.
[37] M. Mooney, A theory of large elastic deformation, J. Appl. Phys. 11 (1940) 582–592.
[38] Large elastic deformations of isotropic materials IV. further developments of the general theory, Philos. Trans. R. Soc. London. Ser. A, Math. Phys. Sci. 241 (1948) 379–397.
[39] T. Zander, M. Dreischarf, A.-K. Timm, W.W. Baumann, H. Schmidt, Impact of material and morphological parameters on the mechanical response of the lumbar spine – a finite element sensitivity study, J. Biomech. 53 (2017) 185–190.

[40] Simcenter Nastran Quick Reference Guide., ((n.d.)).
[41] W. Fan, L.-X. Guo, D. Zhao, Stress analysis of the implants in transforaminal lumbar interbody fusion under static and vibration loadings: a comparison between pedicle screw fixation system with rigid and flexible rods, J. Mater. Sci. Mater. Med. 30 (2019) 118.
[42] A. Shirazi-Adl, M. Parnianpour, Load-bearing and stress analysis of the human spine under a novel wrapping compression loading, Clin. Biomech. 15 (2000) 718–725.
[43] C. Nan, Z. Ma, Y. Liu, L. Ma, J. Li, W. Zhang, Impact of cage position on biomechanical performance of stand-alone lateral lumbar interbody fusion: a finite element analysis, BMC Musculoskelet. Disord. 23 (2022) 920.
[44] R. Bassani, F. Gregori, G. Peretti, Evolution of the anterior approach in lumbar spine fusion, World Neurosurg 131 (2019) 391–398.
[45] Y. Qin, B. Zhao, J. Yuan, C. Xu, J. Su, J. Hao, J. Lv, Y. Wang, Does cage position affect the risk of cage subsidence after oblique lumbar interbody fusion in the osteoporotic lumbar spine: a finite element analysis, World Neurosurg 161 (2022) e220–e228.
[46] Z. Cai, R. Ma, J. Zhang, X. Liu, W. Yang, Z. Wang, B. Cai, X. Xu, Z. Ge, Evaluation of the stability of a novel lateral plate internal fixation: an in vitro biomechanical study, World Neurosurg 158 (2022) e237–e244.
[47] Y. Zheng, L. Chen, J. Shen, B. Gao, X. Huang, Biomechanical evaluation of seven fixation methods to treat pubic symphysis diastasis using finite element analysis, J. Orthop. Surg. Res. 17 (2022) 189.
[48] Y. Ji, Q. Zhang, Y. Song, Q. Hu, G. Fekete, J.S. Baker, Y. Gu, Biomechanical characteristics of 2 different posterior fixation methods of bilateral pedicle screws: a finite element analysis, Medicine (Baltim.) 101 (2022) e30419.
[49] Y. Song, X. Cen, H. Chen, D. Sun, G. Munivrana, K. Bálint, I. Bíró, Y. Gu, The influence of running shoe with different carbon-fiber plate designs on internal foot mechanics: a pilot computational analysis, J. Biomech. 153 (2023) 111597.
[50] X. Cen, Y. Song, P. Yu, D. Sun, J. Simon, I. Bíró, Y. Gu, Effects of plantar fascia stiffness on the internal mechanics of idiopathic pes cavus by finite element analysis: implications for metatarsalgia, Comput. Methods Biomech. Biomed. Engin. (2023) 1–9.
[51] A. Polikeit, S.J. Ferguson, L.P. Nolte, T.E. Orr, The importance of the endplate for interbody cages in the lumbar spine, Eur. Spine J. 12 (2003) 556–561.